Decline in Surface Melt Duration on Larsen C Ice Shelf Revealed by ASCAT Scatterometer

Bevan, Suzanne; Luckman, Adrian; Munneke, Peter Kuipers; Hubbard, Bryn; Kulessa, Bernd; Ashmore, David

Published in:
Earth and Space Science

DOI:
10.1029/2018EA000421

Publication date:
2018

Citation for published version (APA):
Bevan, S., Luckman, A., Munneke, P. K., Hubbard, B., Kulessa, B., & Ashmore, D. (2018). Decline in Surface Melt Duration on Larsen C Ice Shelf Revealed by ASCAT Scatterometer. Earth and Space Science, 5(10), 578-591. https://doi.org/10.1029/2018EA000421

AGU100 ADVANCING EARTH AND SPACE SCIENCE

Earth and Space Science

RESEARCH ARTICLE
10.1029/2018EA000421

Decline in Surface Melt Duration on Larsen C Ice Shelf Revealed by The Advanced Scatterometer (ASCAT)

Suzanne Louise Bevan[1], **Adrian John Luckman**[1], **Peter Kuipers Munneke**[2], **Bryn Hubbard**[3], **Bernd Kulessa**[1], **and David William Ashmore**[4]

[1]Geography Department, College of Science, Swansea University, Swansea, UK, [2]Institute for Marine and Atmospheric research Utrecht, Utrecht University, Utrecht, Netherlands, [3]Centre for Glaciology, Department of Geography and Earth Sciences, Aberystwyth University, Aberystwyth, UK, [4]School of Environmental Sciences, University of Liverpool, Liverpool, UK

Key Points:
- We present the first use of enhanced resolution Advanced Scatterometer (ASCAT) data to identify melt on an Antarctic ice shelf
- The analysis extends the Quick Scatterometer (QuikSCAT) melt record on Larsen C Ice Shelf from 1999–2009 to 2017
- 1999 to 2017 open-shelf melt decreased by 1 or 2 days/year^2, while western inlets saw a similar rate of melt increase

Correspondence to:
S. L. Bevan,
s.l.bevan@swansea.ac.uk

Citation:
Bevan, S. L., Luckman, A. J., Kuipers Munneke, P., Hubbard, B., Kulessa, B., & Ashmore, D. W. (2018). Decline in surface melt duration on Larsen C Ice Shelf revealed by the advanced scatterometer (ASCAT). *Earth and Space Science*, *5*, 578–591. https://doi.org/10.1029/2018EA000421

Received 8 JUN 2018
Accepted 10 SEP 2018
Accepted article online 13 SEP 2018
Published online 3 OCT 2018

Abstract Surface melting has been contributing to the surface lowering and loss of firn air content on Larsen C Ice Shelf since at least the mid-1990s. Where the amount of melting and refreezing is significant, the firn can become impermeable and begin to support ponds of surface meltwater such as have been implicated in ice shelf collapse. Although meteorological station data indicated an increase in melt on the Antarctic Peninsula over the second half of the 20th century, the existing Ku-band Quick Scatterometer (QuikSCAT) time series is too short (1999–2009) to detect any significant 21st century trends. Here we investigate a longer 21st century period by extending the time series to 2017 using the C-band Advanced Scatterometer (ASCAT). We validate our recent observations with in situ weather station data and, using a firn percolation model, explore the sensitivity of scatterometry to water at varying depths in the firn. We find that active microwave C-band (5.6-cm wavelength) instruments can detect water at depths of up to 0.75 m below a frozen firn layer. Our longer scatterometry time series reveals that Larsen C Ice Shelf has experienced a decrease in melt season length of 1–2 days per year over the past 18 years consistent with decreasing summer air temperatures. Only in western inlets, where föhn winds drive melt, has the annual melt duration increased during this period.

Plain Language Summary Antarctic ice shelves form where ice flows from the land and goes afloat on the sea. In recent decades, ice shelves along the Antarctic Peninsula have been disintegrating. Loss of an ice shelf allows faster flow of the land-based ice to the oceans and adds to sea-level rise. One possible cause of ice shelf breakup is increased surface melting; it is therefore important to monitor melt and the best way to do this is from space. We can detect melt from space using microwaves which are scattered back to the spaceborne instrument from the surface. A wet snow surface produces much lower backscatter than a dry one. We investigate trends in the number of days per year when Larsen C Ice Shelf on the Antarctic Peninsula experiences surface melting, using data from a new microwave instrument. On most of the ice shelf, the number of melt days each year has fallen by 1 or 2 days per year since 1999, consistent with decreasing summer air temperatures in this region. However, close to the mountains where the ice shelf is formed the number of melt days is increasing. These locations are where mountain winds known as föhn produce localized increases in surface temperatures.

1. Introduction

Since the advent of satellite altimetry in the early 1990s, volume losses from west Antarctic and Antarctic Peninsula (AP) ice shelves have generally accelerated but have also exhibited a large amount of spatial and temporal variability (Paolo et al., 2015). While not leading directly to sea-level rise, the thinning of ice shelves can lead to grounding-line retreat (Christie et al., 2016; Jenkins et al., 2010; Rignot et al., 2014), increased iceberg calving rates (Liu et al., 2015), and loss of contact with pinning points such as ice rises and rumples (Matsuoka et al., 2015), all of which can reduce the ability of ice shelves to buttress the flow of land ice to the oceans (Dupont & Alley, 2005; Pritchard et al., 2012).

At a mean rate of 3.8 m/decade (1994–2012), eastern AP ice shelves are thinning at only half the rate of those on the western side, but whereas most Antarctic ice shelf thinning is driven by oceanic basal melt (Pritchard

et al., 2012), climate-driven surface processes such as firn compaction appear to be at least equally important on AP ice shelves (Holland et al., 2015). On Larsen C Ice Shelf (LCIS) thinning has progressed southward and the spatial distribution of firn air content reflects a similar north-south gradient in summer melt (Barrand et al., 2013; Holland et al., 2011; Luckman et al., 2014). Superimposed on the north-south gradient is a concentration of melt and firn densification within the north-western inlets in the lee of the Peninsula Mountains (Holland et al., 2011; Luckman et al., 2014).

In these inlets, most notably in Cabinet Inlet, repeated years of melt/refreeze cycles have left the ice shelf surface sufficiently impermeable to support ponds of surface melt water (Alley et al., 2018; Kuipers Munneke et al., 2014; Scambos et al., 2000), a phenomenon which preceded, and may have led to, the collapse of Larsen A, Larsen B, and Wilkins Ice Shelves (Sergienko & Macayeal, 2005; van den Broeke, 2005). Although melt ponds have been observed on LCIS, they are confined to the western inlets where they occupy shallow surface troughs originating at the grounding line (Hubbard et al., 2016; Luckman et al., 2014).

Sums of positive degree days (PDDs) are frequently used to approximate cumulative surface melt; Vaughan (2006) showed that every AP meteorological station showed a statistically significant increase in PDDs over their various observation periods between 1950 and 2000. Long-term trends to 2010 remained positive, albeit at a lower rate (Barrand et al., 2013). A threshold value of 200 melt days per year has been suggested as a limit for ice shelf viability (Fyke et al., 2009; Vaughan, 2006). However, on LCIS summertime can be dominated by calm cloudy conditions and net radiative heating of the surface that eliminates the temperature inversion. Therefore, there can be long periods of surface melt even though the air temperature at 2 m remains below 0°C, meaning that the use of PDDs is likely to underestimate actual snow melt (Kuipers Munneke et al., 2012). Since Trusel et al. (2015) found an exponential rather than linear relationship between surface temperature and meltwater production on ice shelves, being able to detect melt directly using remote sensing would give a better indication of actual conditions at the surface as well as better resolving its spatial variability.

Spaceborne microwave radiometers detect surface melt because microwave brightness temperatures rise sharply when liquid water is present in the snowpack. We emphasize here that remotely sensing melt refers to detecting the presence of liquid water rather than the process of melting, although the two can be related (van den Broeke et al., 2009). Melt detection algorithms commonly rely on microwave brightness temperatures exceeding some threshold above winter (dry snow) temperatures (e.g., Ashcraft & Long, 2006; Tedesco, 2009; Torinesi et al., 2003). Alternatively a cross-polarization gradient ratio allows a threshold to be set that does not depend on winter temperatures (Abdalati & Steffen, 1995). Passive microwave data, available from 1979, revealed no long-term trends in melt extent or duration for the AP from 1980 to 2005 (Picard & Fily, 2006).

Active microwave sensors are another instrument capable of detecting surface melt. From 1999 to 2009 scatterometer data from the SeaWinds instrument on the Quick Scatterometer (QuikSCAT) mission allowed the detection of melt at a much improved spatial resolution (2.225–4.45 km) compared with that of passive microwave radiometers (25 km). Snowmelt detection in scatterometer data relies on the large decrease in backscatter caused by the presence of small amounts of liquid water in the snowpack.

By using enhanced resolution products (Early & Long, 2001; Long & Hicks, 2010), Barrand et al. (2013) were able to map melt indices such as melt extent, onset date, and melt duration for the whole AP at a spatial resolution of 2.225 km. The study found no clear trends in either melt onset day or melt duration but did identify a high degree of interannual variability, particularly on ice shelves. The association of surface melt with ice shelf breakup emphasizes the need to continue the remotely sensed melt record beyond 2009, both to monitor the evolution of melt and to validate the energy and mass balance models that elucidate the processes and components of melt.

QuikSCAT ceased operating at the end of 2009, so following the example of Mortin et al. (2014) who used enhanced resolution data from the Advanced SCATterometer (ASCAT) instrument to extend the record of melt-refreeze transitions over Arctic sea ice, we turn to ASCAT data to extend the record of AP ice shelf melt. Concentrating on LCIS where we have in situ surface energy balance (SEB) data based on automatic weather station observations, we compare QuikSCAT and ASCAT sensitivities to melt and validate the ASCAT melt detection capability by comparing a time series of backscatter intensity with profiles of snowpack liquid water generated using the SEB model. We then (i) repeat the QuikSCAT time window and (ii) extend the analysis of surface melt to 2017, using the enhanced resolution ASCAT data. Using the extended time series, we test

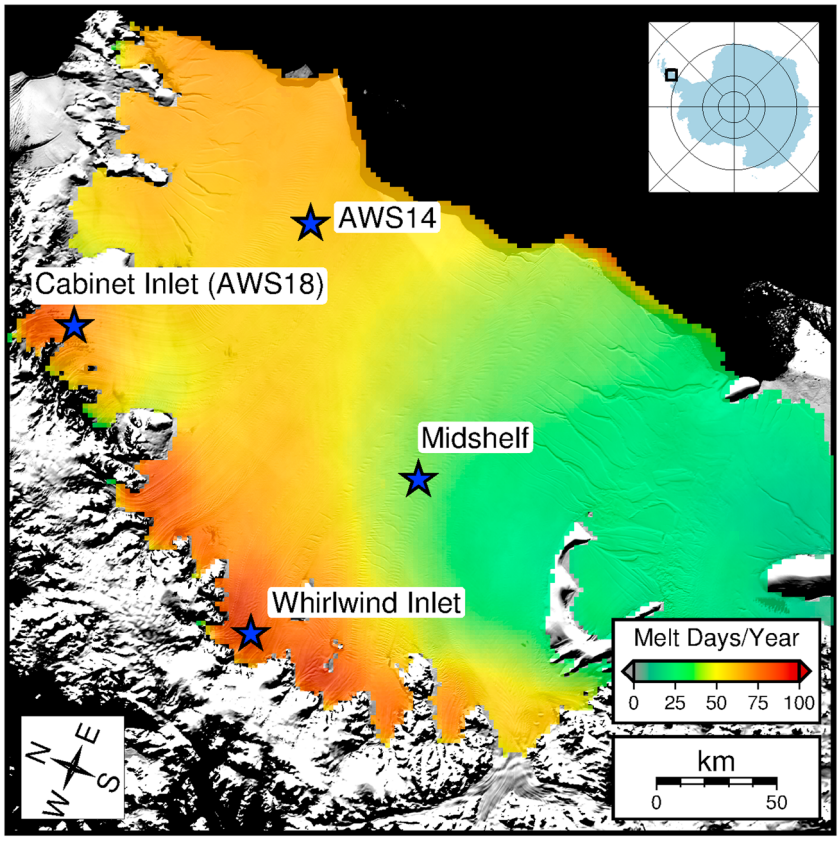

Figure 1. Mean annual number of melt days from 1999/2000 to 2016/2017 based on QuikSCAT morning (1999–2009) and Advanced Scatterometer (ASCAT) (2009–2017). The blue stars mark the locations where backscatter values were extracted for Figures 4, 5, and 7. The background is from the Mosaic of Antarctica (MOA2009; Haran et al., 2014; Scambos et al., 2007).

for linear trends in melt duration over the 1999–2017 period and investigate possible links with large-scale atmospheric indices.

2. Data and Methodology

2.1. Melt From Scatterometer Data

Melt detection is based on enhanced-resolution radar backscatter (σ^0) data from the QuikSCAT (1999–2009) and ASCAT (2008–2017) instruments. The data are available from Brigham Young University (www.scp.byu.edu) Microwave Earth Remote Sensing Laboratory where resolution has been enhanced by application of the Scatterometer Image Reconstruction algorithm that allows the combination of multiple pass, irregularly spaced data into higher-resolution gridded images (Early & Long, 2001).

The QuikSCAT instrument operates at Ku-band (13.4 GHz); both vertical and horizontal polarization data are acquired, and the pixel size ranges from 2.225 to 4.45 km depending on the temporal processing. The ASCAT instrument is a C-band (5.255 GHz) scatterometer; the antennae are vertically polarized only, and the Scatterometer Image Reconstruction with filtering product has a pixel size of 4.45 km. As melt/refreeze is likely to follow a diurnal cycle, with refreezing occurring at night, the midafternoon local time of day QuikSCAT, so-called qnsh (noon, horizontally polarized) or qnsv (noon,vertically polarized), products (2.225-km resolution) are normally chosen for melt studies to maximize the likelihood of melt detection (Barrand et al., 2013; Trusel et al., 2012).

Here we also investigate the use of the morning vertical polarization product (qmsv, resolution of 4.45 km) anticipating that it will have a similar chance of observing melt to the daily all-pass (msfa) ASCAT product. ASCAT does not acquire data over Antarctica in the afternoon, only in the morning and evening; the msfa product combines all data acquired within a single 24-hr period. From this point we refer to the QuikSCAT

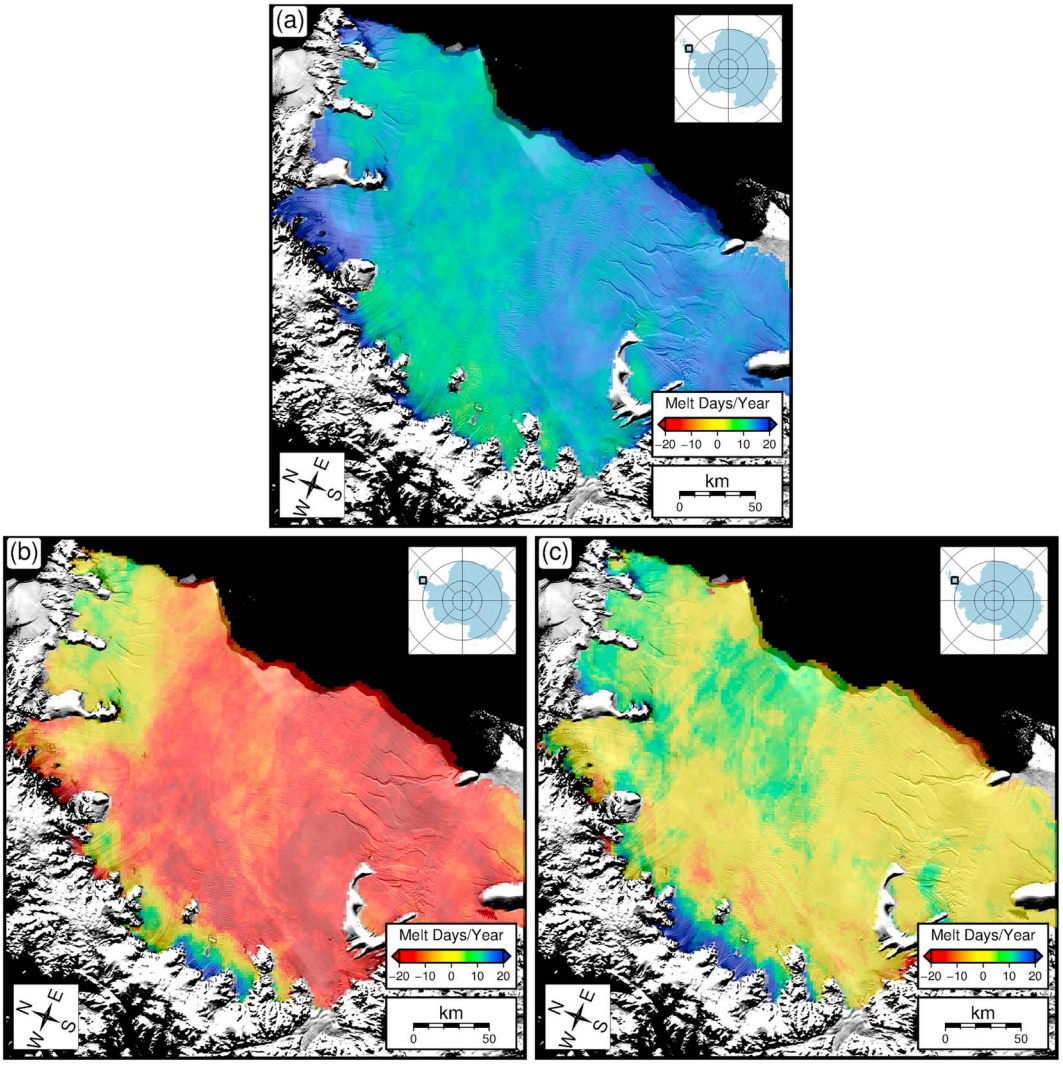

Figure 2. (a) Differences between QuikSCAT noon and QuikSCAT morning melt days over the 10-year QuikSCAT record. Difference in 2008/2009 melt days (b) Advanced Scatterometer (ASCAT) minus QuikSCAT noon and (c) ASCAT SCATterometer minus QuikSCAT morning.

qnsh product as QuikSCAT noon and the qmsv product as QuikSCAT morning. Consistency between products is important if we are to construct a combined time series and test for trends in melt. The issue of observation time was addressed by Picard and Fily (2006) when they calculated regional trends in Antarctic cumulative melt surface (CMS) based on microwave radiometer data from different instruments and missions. They fitted a sinusoidal model to the diurnal variation in CMS using instrument overlap periods. For the AP region the amplitude of the diurnal variation in CMS was small in comparison with the interannual variation.

Similar to other studies (Barrand et al., 2013; Trusel et al., 2012; Wismann, 2000), we assume the presence of liquid water when σ^0 falls below the previous winter mean by a fixed threshold. A higher percentage of liquid water content (LWC) and thicker wet snow layers will result in a more significant fall in σ^0. For the QuikSCAT data we used a threshold of 3 dB as modeled by Ashcraft and Long (2006) to represent the response to a LWC of 3% in a snow depth of 3.8 cm. The lower frequency of the ASCAT C-band means that the same amount and depth of liquid water results in a lower absorption—a lower threshold is therefore appropriate for the ASCAT measurements. Ashcraft and Long (2006) arrived at a threshold of 2.7 dB for the ERS C-band scatterometer via an empirical comparison with QuikSCAT, and we adopt the same threshold in this study. Using the ERS C-band σ^0 to detect melt on Greenland, Wismann (2000) found that a 3-dB threshold corresponded to a LWC of 0.5% and a 7-cm snow layer but that choosing threshold values of 2 to 4 dB did not significantly change the pattern or observed interannual variability of melt. We define the austral melt year to begin on August 1st, with June,

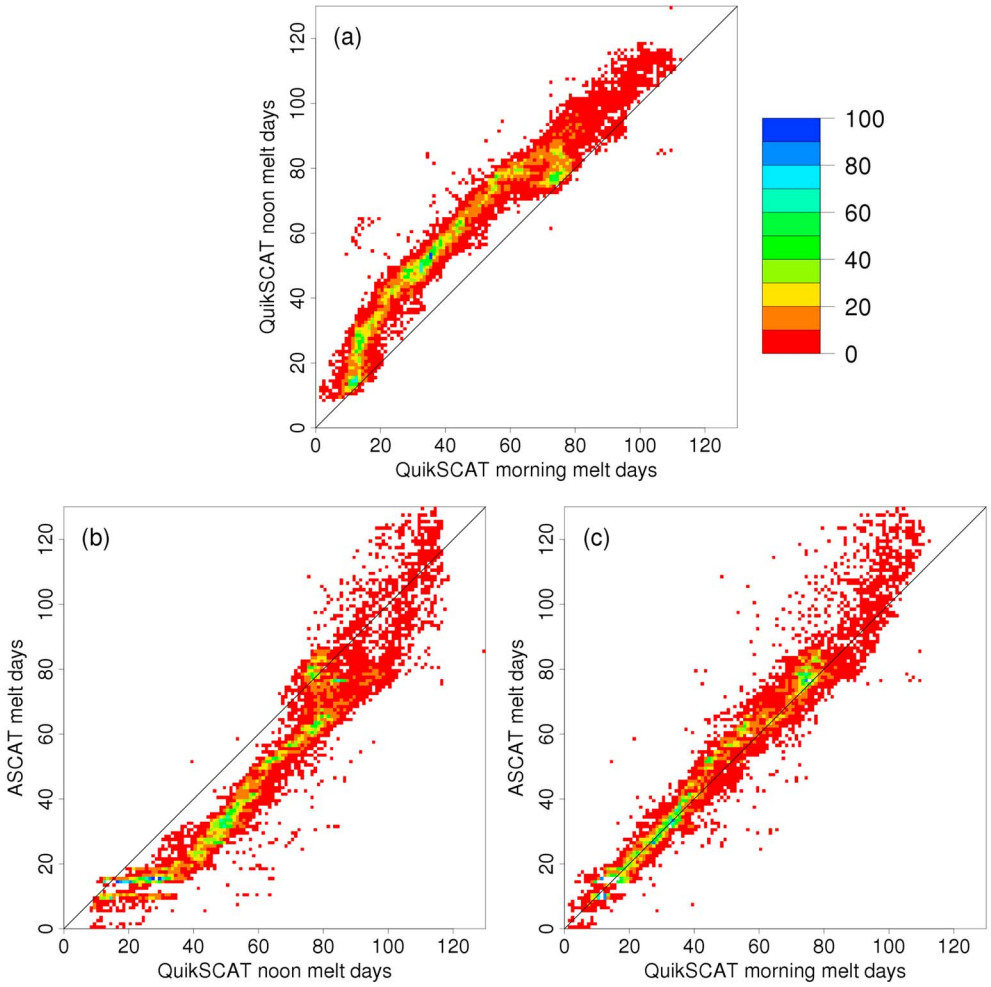

Figure 3. The 2008/2009 melt-day comparison of the whole ice shelf. (a) QuikSCAT noon against QuikSCAT morning, (b) ASCAT against QuikSCAT noon, and (c) ASCAT against QuikSCAT morning. A point for every pixel on LCIS. ASCAT = Advanced Scatterometer.

July and August being the winter months for the purpose of calculating the winter-mean backscatter. Total annual melt days is the sum of all days during which melt is detected at each grid location. Both data sets have occasional days of missing data amounting to 36 days in total for QuikSCAT and 30 days for ASCAT; the longest consecutive gap is in the ASCAT data and is 5 days between 28 March and 3 April 2010. On these days we assume a melt condition equal to that of the preceding day.

A number of metrics have been used to report remotely sensed melt, including melt duration (the number of melt days per year), melt extent (the total area affected by melt in a given year), and melt intensity (the product of melt duration and melt extent, analogous to CMS). Also reported for some regions are melt onset and melt end; we do not report the latter metrics in this study as it is not uncommon on LCIS for there to be periods of melt outside of the continuous summer melt period that are associated with föhn wind events (Kuipers Munneke et al., 2018; Luckman et al., 2014)

2.1.1. QuikSCAT/ASCAT Comparison

For the 2008/2009 melt season we have data from both QuikSCAT and ASCAT and we use this period to compare the ability of each instrument to detect melt. We look at the difference in melt duration across the ice shelf detected by QuikSCAT noon, QuikSCAT morning, and ASCAT. We also compare time series of backscatter for four sites (Figure 1): Cabinet Inlet (the location of automatic weather station AWS18, 66.4°S, 63.4°W), the location of AWS14 (67.0°S, 61.5°W), Whirlwind Inlet (67.5°S, 65.3°W), and a midshelf location (67.8°S, 63.2°W).

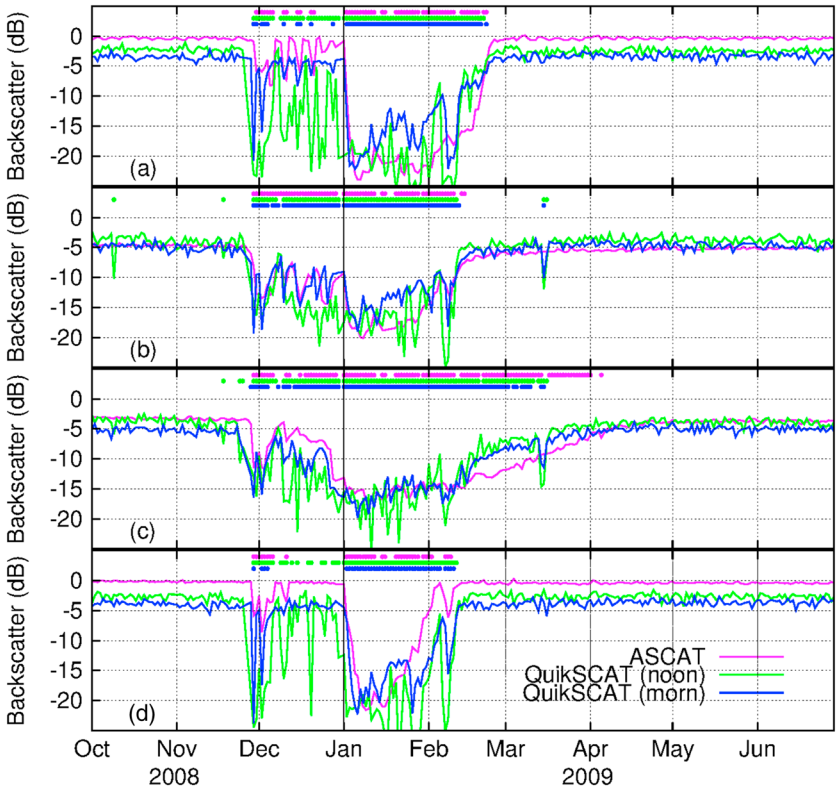

Figure 4. Pixel backscatter for QuikSCAT noon, QuikSCAT morning, and Advanced Scatterometer (ASCAT). The upper lines of dots indicate when a melt day was detected. (a) AWS14, (b) Cabinet Inlet (AWS18), (c) Whirlwind Inlet, and (d) midshelf location. See Figure 1 for locations.

2.2. In Situ Validation Using Modeled Liquid-Water Profiles

To evaluate the ability of ASCAT to detect the presence of liquid water in snow, we use a time series of vertical profiles of liquid water from the subsurface module of an SEB model (Kuipers Munneke et al., 2012). The model is forced by 30-min surface observations from AWS18 in Cabinet Inlet (Figure 1), made between 24 November 2014 and 13 November 2017. Surface meltwater is allowed to percolate into a multilayer snowpack and can be retained in a snow layer as long as the pore space is not saturated. Otherwise, the meltwater percolates to the next layer instantly (the tipping bucket method). It can refreeze if snow temperature allows, and the release of latent heat upon refreezing warms the snow layer. Snow density is simply prescribed as a vertical profile constant in time, based on snow-pit observations.

2.3. Melt Trend

In spite of both the QuikSCAT morning and ASCAT all-pass products having the potential to underestimate melt in comparison with QuikSCAT noon, particularly in locations where the presence of meltwater varies diurnally, we use the similarity we find in their sensitivities to melt to construct an extended time series of LCIS annual melt duration.

We calculate the linear trend in melt duration on the ice shelf from 1999 to 2017, using the QuikSCAT morning data up to and including the overlapping 2008/2009 melt season and ASCAT data for the remainder of the period. We attempt to test the impact on the computed trends of the instrument switch from 2009/2010 onward by also calculating the trends using a bias-corrected ASCAT time series. The bias correction involves scaling every ASCAT melt duration value by the QuikSCAT morning to ASCAT ratio from the overlap period, on a pixel-by-pixel basis. This method of bias correction applies a larger absolute adjustment to high-melt years, reflecting the spatial correlation between bias and melt duration (Figures 2c and 3c).

The Southern Annular Mode (SAM) index, defined as the zonal pressure difference between the latitudes of 40°S and 65°S (Marshall, 2003), reflects the strength of the westerly atmospheric circulation in the middle-high latitudes. A positive SAM is associated with strong westerly winds, including across the AP. On eastern AP ice shelves, particularly close to the mountains, the enhanced westerlies can lead to surface warming and melt

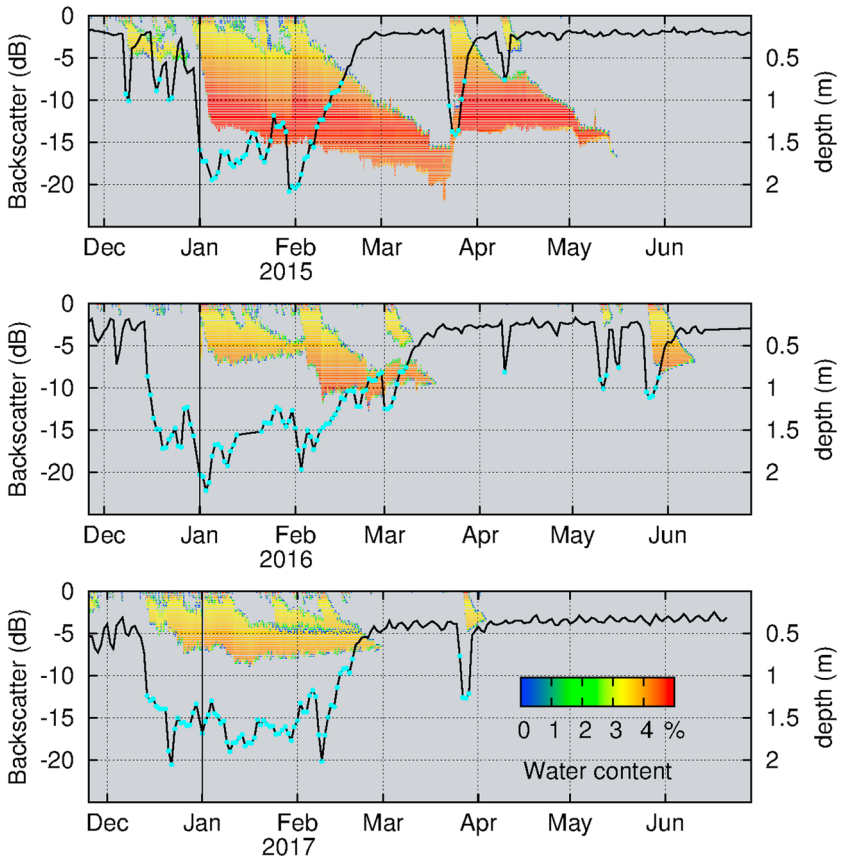

Figure 5. Profiles of percentage liquid water content from the surface energy balance model for AWS18 (Figure 1). The black line is the Advanced Scatterometer (ASCAT) backscatter (dB) for the same location with days classified as melt days marked in cyan.

due to the föhn wind effect (Cape et al., 2015; Elvidge et al., 2015; Luckman et al., 2014). To test the sensitivity of LCIS melt to large-scale atmospheric dynamics, we calculate the correlation coefficients between austral-year and summer (combined December, January, and February) SAM indices (defined on the basis of air pressure observations as in Marshall, 2003) and melt duration on a pixel-by-pixel basis. We also calculate the correlation between SAM indices and ice shelf annual melt index.

3. Results

3.1. Melt Detection

3.1.1. QuikSCAT/ASCAT Comparison

Over the full 10-year QuikSCAT record the mean difference in annual melt duration detected by QuikSCAT noon and QuikSCAT morning is 14 days (standard deviation 3 days), with the noon value exceeding the morning value over the entire ice shelf (Figures 2a); in 2008/2009 the mean difference is 13.5 days (standard deviation 6.4 days; Figure 3a). In 2008/2009, ASCAT melt duration is predominantly less than QuikSCAT noon except in the very north and in the south-western inlets (Figures 2b). The mean ASCAT-QuikSCAT noon value is −11.4 days (standard deviation 8.0 days; Figure 3b). Note that even though QuikSCAT noon detects more melt than QuikSCAT morning, there are places where it detects less than ASCAT. As expected, a better agreement is found between ASCAT and QuikSCAT morning, where ASCAT generally exceeds QuikSCAT morning over the northern part of the ice shelf and most strongly in the south-western inlets where the difference can be up to 30 days (Figures 2c). On the open shelf the agreement is mostly ±5 days. Mean ASCAT minus QuikSCAT morning is 2.1 days (standard deviation 5.0 days; Figure 3c).

For the 2008/2009 melt season the melt index for QuikSCAT noon is 4.2×10^6 melt days km^2, for QuikSCAT morning it is 3.3×10^6 melt days km^2, and for ASCAT it is 3.4×10^6 melt days km^2.

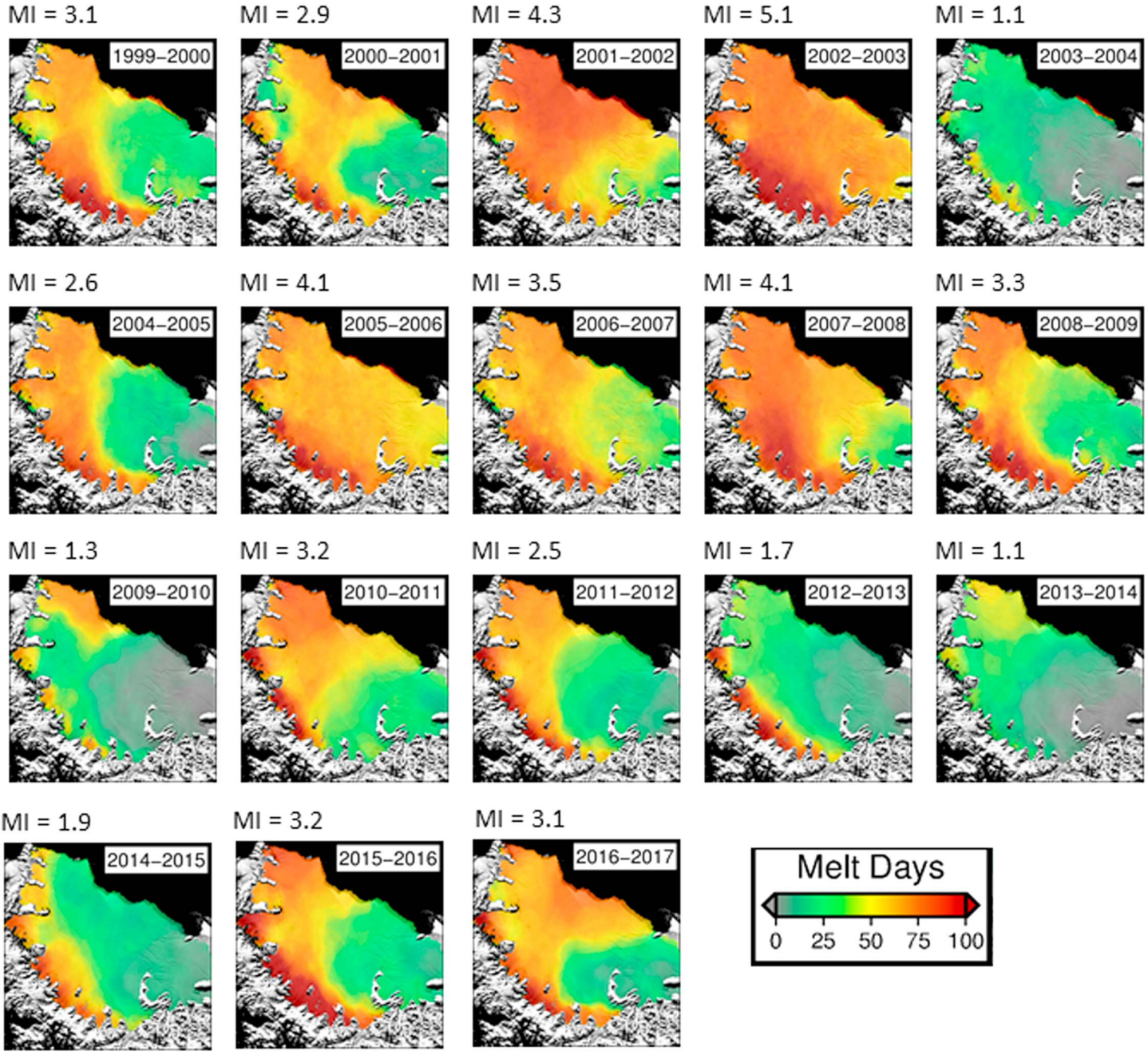

Figure 6. Annual number of melt days from 1999/2000 to 2016/2017 based on QuikSCAT morning (1999–2009) and Advanced Scatterometer (ASCAT) (2009–2017). The melt index (MI) is in 10^6 melt days km^2.

Time series of backscatter at four locations (Figure 1) during the 2008/2009 melt season show which days each instrument indicated the presence of melt (Figure 4). At AWS14, QuikSCAT noon backscatter indicated 81 days of melt, QuikSCAT morning 62 days, and ASCAT 65 days. Melt begins in December with backscatter oscillating above and below the melt threshold, and only the QuikSCAT noon product detects near continuous melt. Backscatter then drops sharply at the beginning of January 2009 and stays low until 23 February (Figure 4a), and all instruments record continuous melt. Note that the intermittent gaps in the ASCAT melt symbols for January and February in all four panels of Figure 4 are due to missing data, but the algorithm counts these as melt days. In Cabinet Inlet QuikSCAT noon detects 80 days of melt, QuikSCAT morning 77 days, and ASCAT detects 76, the time profile of melt is similar to AWS14 although the melt in December has a stronger signature (Figure 4b). Both QuikSCAT morning and ASCAT miss an October melt day and a weak December one which were detected by QuikSCAT noon. The short melt event missed by ASCAT in March is due to missing data. In

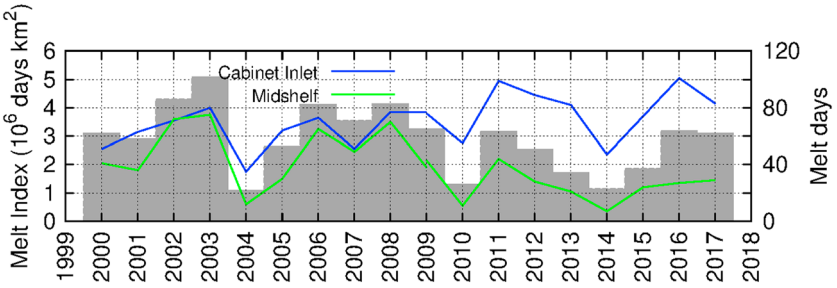

Figure 7. Ice shelf wide melt index and melt days for Cabinet Inlet and midshelf (see Figure 1 for locations) based on QuikSCAT morning (1999–2009) and Advanced Scatterometer (ASCAT) (2009–2017). Both ASCAT and QuikSCAT morning are shown for 2008/2009 melt days.

Whirlwind Inlet, although onset of melt is quite clear and abrupt, freezeup is much more gradual (Figure 4c), QuikSCAT noon detects 113 days of melt, QuikSCAT morning 98 days, and ASCAT detects 115 days. The close agreement in total melt days between ASCAT and QuikSCAT noon is because although ASCAT continues to detect melt into April, 18 days after QuikSCAT noon, ASCAT misses some days in November and December which were detected by QuikSCAT noon. At the midshelf location QuikSCAT noon and QuikSCAT morning detect 44 and 38 days, respectively, and ASCAT detects 43 days (Figure 4c). Start and end dates are in good agreement across all three sensors, but only QuikSCAT noon picks up much melt during December.

3.2. Comparison With Modeled Liquid-Water Profiles

Throughout the melt seasons of 2014/2015, 2015/2016, and 2016/2017 the SEB model at AWS18 shows that melt events at the surface generate water that percolates down through the snowpack over the following days and weeks, reaching depths of up to 2 m and concentrations of up to 4.5% (Figure 5). There appear to be periods of many weeks with no melting occurring at the surface but with liquid water present at depth. During such periods the ASCAT backscatter signal continues to be attenuated and melt days are recorded, for example, on 16 February 2016 a melt day is recorded but all the liquid water present is below 0.75 m. As the freeze front gradually descends below 0.75 m the backscatter recovers. In 2015/2016 and 2016/2017 the intensity of melt is much lower but the radar backscatter still responds. Melt days are also detected when the model does not indicate any melt, such as during late December 2015 and during April 2016. Three early winter melt events occur during May 2016 that are picked up by the scatterometer.

3.2.1. Melt Time Series and Trends

With earlier results indicating that the QuikSCAT morning product provides the best consistency with the ASCAT product in terms of detecting annual melt duration we chose to continue our investigation into melt trends using the QuikSCAT morning product. We calculate linear trends in melt using QuikSCAT morning for the 1999/2000 to 2008/2009 melt seasons inclusive and ASCAT for 2009/2010 to 2016/2017, even though both products may be underestimating total annual melt over much of the ice shelf. Hence, the results presented in Figures 1, 6, 7, and 8 are based on QuikSCAT morning combined with ASCAT data.

The 1999–2017 melt patterns on LCIS are characterized by a south-to-north increase with enhanced melt also occurring in the western inlets (Figures 1 and 6), as discussed by Luckman et al. (2014). Close to the Peninsula Mountains, which lie along the western edge of the ice shelf, melt duration can exceed 100 days a year. Even in years when there is very little melt on the open shelf, such as 2003/2004, the inlets feature melt durations of up to 65 days (Figure 6).

The 1999/2000 to 2016/2017 mean LCIS melt index is 2.89×10^6 melt days km^2, but there is a lot of interannual variability with melt indices ranging from 1.09×10^6 melt days km^2 in 2003/2004 to 5.09×10^6 in 2002/2003 (Figures 6 and 7). There is no significant trend in melt index over the full time period. Time series of annual melt days for Cabinet Inlet and for a midshelf location (see Figure 1 for locations) indicate opposing trends from 2008/2009, with Cabinet Inlet appearing to experience increasing melt and the open shelf experiencing decreasing melt. Figure 7 shows that the LCIS melt index may be starting to increase toward the end of the period; recalculating the trend excluding the final 2 years results in a decreasing trend significant at 95%.

In spite of the large interannual variability, over the extended 1999/2000 to 2016/2017 period, there has been an annual decrease of 1 to 2 melt days per year over most of LCIS (Figure 8a). The trend is significant at 90% (95%) over about 33% (6%) of the ice shelf, mostly over the southern parts. In the western inlets there has

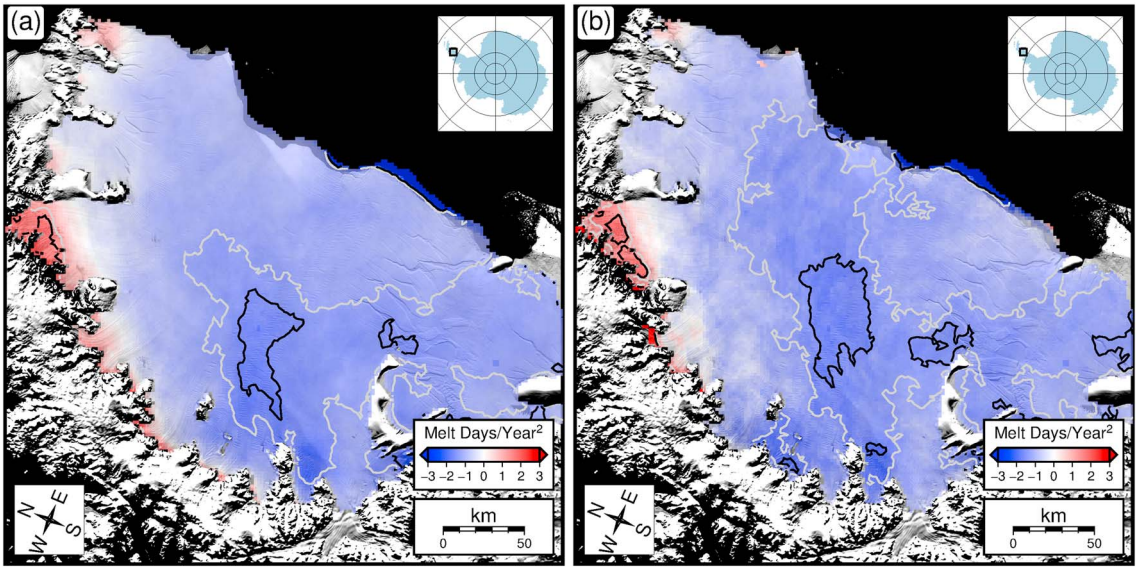

Figure 8. (a) Linear trend in annual melt days/year^2 from 1999/2000 to 2016/17 combining QuikSCAT morning with Advanced Scatterometer (ASCAT). White contour marks the areas significant at 90%, black contour the areas significant at 95%. (b) Trends based on a linear-ratio bias correction for ASCAT melt durations. See text for further details.

been an increasing trend, which is significant (at 95%) within Cabinet Inlet. Trends using the bias-corrected ASCAT melt time series are similar, suggesting that the instrument switch has had little impact, with the area of decreasing trend covering 40% (90% significance) and 10% (95% significance) of the ice shelf and the area of increasing trend extending slightly further south (Figure 8b). Similar to the melt-index result, if the final 2 years of the series are excluded, the decline in melt becomes more significant. Thus, from 1999/2000 to 2014/2015, 35% of the ice shelf experiences a decrease in annual melt of 2 or 3 days per year, significant at the 95% level (using the non-bias-corrected ASCAT data). Cabinet Inlet still experiences an increasing trend in melt days.

Over the 1999–2017 period we found no significant correlation between annual or summer SAM indices and melt duration or melt index. Neither did we find any trend in either of the SAM indices although they remained predominantly positive.

4. Discussion

4.1. Melt Detection and Validation

In discussing melt based on the analysis of radar scatterometer data we are referring to the detection of liquid water at the surface or within the snowpack, rather than active surface melt events. The dielectric permittivity of ice is low so that for dry snow the radar backscatter function is dominated by volume scattering. The contrastingly high dielectric permittivity of liquid water means that even a small amount of liquid water anywhere within the penetration depth will effectively absorb the microwave radiation and attenuate the backscatter. The detection of subsurface liquid water is clearly shown in Figure 5 when backscatter drop exceeds the threshold set to indicate melt even when, according to the model, there is no liquid water at the surface. The reduction in penetration depth, indicated by the reduced sensitivity to subsurface liquid water as the season continues, may be a consequence of the changing fabric of the upper snowpack as it undergoes a number of melt/refreeze cycles and the mean size of ice crystals increases.

As expected, based on a probable diurnal cycle with melt peaking in the afternoon, the QuikSCAT noon melt duration was greater on average than the morning product by about 10%. Spatial variability in the mean difference (Figure 2a) is probably due to spatial variability in melt intensity. The difference between the two products is lower in areas that experience greater melt (Figure 3a) where liquid water can persist within the snowpack even if the surface refreezes. In Cabinet Inlet, where föhn-driven melt is not dependent on radiative heating, QuikSCAT morning and noon products are very similar for 2008/2009 (Figure 4b), although in the long-term mean the noon melt duration is clearly longer (Figure 2a).

While the agreement between QuikSCAT and ASCAT is better for the QuikSCAT morning product on which we base the time series, there are still some clear differences (Figure 2c). Generally, in areas of long melt duration, such as to the north of the ice shelf and in the inlets, ASCAT tends to detect more melt days than QuikSCAT morning. Conversely, in areas where melt duration is shorter, QuikSCAT morning detects more melt than ASCAT. As both observations include morning data the differences in melt detection are probably caused by the different operating wavelengths.

At ASCAT C-band wavelengths (5.6 cm) the same depth and volume of water result in less absorption than at QuikSCAT Ku-band wavelengths (2.2 cm), so that the theoretical estimate of a threshold equivalent to the 3 dB used for QuikSCAT would be only 1 dB (Ashcraft & Long, 2006). However, Ashcraft and Long (2006) found that 1 dB gave too many false melt detections and chose a 2.7-dB threshold as it gave the best empirical agreement between ERS scatterometer (an earlier C-band instrument) detected melt and QuikSCAT detected melt. This threshold required a theoretical wet snow depth of about twice that required for QuikSCAT melt; hence, our use of a 2.7-dB threshold may also require a greater intensity of melt in order for initial detection to occur compared with QuikSCAT. This difference in sensitivity would explain why in lower melt regions, such as on the southern portion of the ice shelf, ASCAT detects fewer melt days than QuikSCAT morning (Figure 2c).

As well as depending on the LWC, the penetration depth depends on the wavelength of the incident radiation. For microwave radiation scattered by snow grains, longer wavelengths experience increased Rayleigh scattering and consequently reduced penetration depths (Nghiem & Tsai, 2001). When refreeze occurs, the greater penetration depth at ASCAT wavelengths allows the continued detection of subsurface liquid water after the surface has refrozen and when QuikSCAT backscatter has recovered. The delayed detection of refreeze initiated at the surface may explain why ASCAT melt duration exceeds QuikSCAT melt duration in areas where melt has been more intense and/or prolonged and meltwater has percolated to a greater depth, such as the northern half of the shelf and the inlet regions. A particularly slow refreeze and recovery of winter backscatter is shown in Whirlwind Inlet, where ASCAT's greater penetration depth means that backscatter continues to be attenuated relative to the winter mean and ASCAT records a greater number of melt days (Figure 4b).

Returning to the comparison of the commonly used QuikSCAT noon product with the currently available ASCAT product, we note that the differing observation times means that ASCAT will on average underestimate melt. However, where melt is intense the increase in penetration depth owing to the longer ASCAT wavelength may compensate for the local time of day effect by being more sensitive to persistent subsurface liquid water. A close inspection of the SEB LWC (Figure 5) indicates that at shallow depths where a melt-refreeze diurnal cycle occurs, ASCAT continues to indicate melt owing to its ability to detect subsurface liquid water.

While we can conclude that a particular sensor, overpass time, or algorithm has missed a melt day if either or both of the other products we have used detect melt, all products are best estimates with the data available. Ideally, we would require continuous observations at a wavelength that penetrates to detect subsurface liquid water at any depth included in a definition of surface melt.

4.2. Melt Trends and the Large-Scale Modes of Atmospheric Flow

The decreasing trend in annual melt duration over much of LCIS (Figure 8) over 2000–2016 is likely in response to decreasing 21st century AP surface air temperatures (Turner et al., 2016). Data from Bellingshausen, O'Higgins, Esperanza, Marambio, Verndadsky, and Rothera weather stations show the greatest cooling (0.72 °C per decade) to have occurred in austral summer. At the same time, the midlatitude jet has been strengthening, reflecting a trend toward more positive values of the SAM index. This apparent contradiction to the idea that SAM and AP temperature are positively correlated can be reconciled by the following two arguments: (1) the correlation between SAM and AP temperature is strong and significant in all seasons except in summer (Cape et al., 2015), which is when the majority of melt occurs. Thus, the relation between SAM and LCIS surface melt is expected to be weak; (2) while the midlatitude jet strengthened, the meanders in the jet also shifted along-flow. This led to a summertime mean sea-level pressure decrease over the South Atlantic and an increase over the Bellingshausen Sea to the west of the AP. The consequent enhanced cyclonic circulation over the South Atlantic led to stronger east to south-easterly winds advecting sea ice toward the eastern AP (Turner et al., 2016) and restricting the landward flux of oceanic heat. In other words, although the positive SAM index during this period would suggest stronger westerly flow and therefore increased AP temperatures, departures from the mean annular pattern of flow in fact led to cooler temperatures.

The period used in this study to calculate trends is somewhat arbitrary, being determined by the number of years of available data; in addition, interannual variability is high. By excluding the final 2 years of data the decreasing melt trends become statistically significant over a greater part of the ice shelf, and the period exactly matches that over which Turner et al. (2016) detected decreasing AP surface air temperatures. Speculatively, the last 2 or 3 years of LCIS melt index indicate that here the period of decreasing ice shelf summer melt may be ending (Figure 7); Wiesenekker et al. (2018) note an increase in Cabinet Inlet föhn events during 2015 and 2016.

The downward trend in observed surface melt is consistent with recent (2009–2017) increases in LCIS surface elevation within a 1992–2017 satellite radar altimetry record (Adusumilli et al., 2018). Surface mass balance (van Wessem et al., 2018) and firn density models (Ligtenberg et al., 2011) allowed this elevation increase to be attributed to increased firn-air content following reduced surface melt in agreement with our observations, rather than to increased snowfall.

The small regions of increasing melt we observe are close to the mountains (Figure 8) in the domain affected by föhn winds descending from the AP mountains (Elvidge et al., 2015; Luckman et al., 2014; Wiesenekker et al., 2018). The winds bring episodes of positive surface air temperatures and clear skies, even in the winter (Kuipers Munneke et al., 2018; Wiesenekker et al., 2018), and therefore, the melt trend is less likely to be driven by the summer circulation that led to cooling on the rest of the shelf.

5. Conclusions

In this work we investigate the use of ASCAT scatterometer data to extend the melt record on LCIS beyond the QuikSCAT (1999–2009) era. Differing overpass times mean that the best continuity in melt products is found by using QuikSCAT morning and ASCAT all-pass data. While both these products are likely to underestimate melt where melt has a diurnal signal, the effect is reduced in high-melt regions due to the persistence of liquid water within the snowpack and the ability of microwaves to penetrate beneath the surface. We have shown that at ASCAT wavelengths (C-band, 5.6 cm) early-season subsurface liquid water is detectable at depths of up to 0.75 m but that the depth to which subsurface water can be detected may change throughout the melt season.

Understanding the characteristics of melt detection using ASCAT data, and how it compares with QuikSCAT melt detection, is particularly valuable as the ASCAT instrument series is likely to continue to at least 2020, with instruments currently operating on METOP-A and METOP-B, and METOP-C planned for launch in 2018.

We found statistically significant decreasing trends in melt duration during 1999–2017 of between 1 and 2 days per year over parts of LCIS consistent with decreasing AP air temperatures. Truncating the time series to match the exact interval over which the air temperature and trends were calculated increased the significance of, and areas covered by, the trends. The trends are likely part of the natural decadal variability in climate for this region. In the inlets close to the mountains, which are regions affected by föhn winds, we detected a statistically significant increase in melt duration of up to 2 days per year.

Acknowledgments
The research was funded by the Natural Environment Research Council (NERC) grants NE/L006707/1 and NE/L005409/1. Grids of melt duration, onset date, and end date for the Antarctic Peninsula region are available at the UK Polar Data Centre (https://doi.org/10.5285/e3616d28-759e-4cca-8fae-fe398f9552ba). Output from AWS18 is also available at the UK Polar Data Centre (https://doi.org/10.5285/05c9124b-7119-4d99-8e17-ab754eb3f51c). Enhanced-resolution radar backscatter (σ^0) QuikSCAT (1999–2009) and ASCAT (2008–2017) data are available from Brigham Young University (www.scp.byu.edu) Microwave Earth Remote Sensing Laboratory (MERS).

References

Abdalati, W., & Steffen, K. (1995). Passive microwave-derived snow melt regions on the Greenland Ice Sheet. *Geophysical Research Letters*, *22*(7), 787–790. https://doi.org/10.1029/95GL00433

Adusumilli, S., Fricker, H. A., Siegfried, M. R., Padman, L., Paolo, F. S., & Ligtenberg, S. R. M. (2018). Variable basal melt rates of Antarctic Peninsula Ice Shelves, 1994–2016. *Geophysical Research Letters*, *45*, 4086–4095. https://doi.org/10.1002/2017gl076652

Alley, K. E., Scambos, T. A., Miller, J. Z., Long, D. G., & MacFerrin, M. (2018). Quantifying vulnerability of Antarctic ice shelves to hydrofracture using microwave scattering properties. *Remote Sensing of Environment*, *210*, 297–306. https://doi.org/10.1016/j.rse.2018.03.025

Ashcraft, I. S., & Long, D. G. (2006). Comparison of methods for melt detection over Greenland using active and passive microwave measurements. *International Journal of Remote Sensing*, *27*, 2469–2488. https://doi.org/10.1080/01431160500534465

Barrand, N. E., Vaughan, D. G., Steiner, N., Tedesco, M., Kuipers Munneke, P., van den Broeke, M. R., & Hosking, J. S. (2013). Trends in Antarctic Peninsula surface melting conditions from observations and regional climate modeling. *Journal of Geophysical Research: Earth Surface*, *118*, 315–330. https://doi.org/10.1029/2012JF002559

Cape, M. R., Vernet, M., Skvarca, P., Marinsek, S., Scambos, T., & Domack, E. (2015). Foehn winds link climate-driven warming to ice shelf evolution in Antarctica. *Journal of Geophysical Research: Atmospheres*, *120*, 11,037–11,057. https://doi.org/10.1002/2015jd023465

Christie, F. D. W., Bingham, R. G., Gourmelen, N., Tett, S. F. B., & Muto, A. (2016). Four-decade record of pervasive grounding line retreat along the Bellingshausen margin of West Antarctica. *Geophysical Research Letters*, *43*, 5741–5749. https://doi.org/10.1002/2016gl068972

Dupont, T. K., & Alley, R. B. (2005). Assessment of the importance of ice-shelf buttressing to ice-sheet flow. *Geophysical Research Letters*, *32*, L04503. https://doi.org/10.1029/2004GL022024

Early, D. S., & Long, D. G. (2001). Image reconstruction and enhanced resolution imaging from irregular samples. *IEEE Transactions on Geoscience and Remote Sensing*, *39*(2), 291–302. https://doi.org/10.1109/36.905237

Elvidge, A. D., Renfrew, I. A., King, J. C., Orr, A., Lachlan-Cope, T. A., Weeks, M., & Gray, S. L. (2015). Foehn jets over the Larsen C Ice Shelf, Antarctica. *Quarterly Journal of the Royal Meteorological Society*, *141*, 698–713. https://doi.org/10.1002/qj.2382

Fyke, J. G., Carter, L., Mackintosh, A., Weaver, A. J., & Meissner, K. J. (2009). Surface melting over ice shelves and ice sheets as assessed from modeled surface air temperatures. *Journal of Climate*, *23*, 1929–1936. https://doi.org/10.1175/2009jcli3122.1

Haran, T., Bohlander, J., Scambos, T., Painter, T., & Fahnestock, M. (2014). MODIS mosaic of Antarctica 2008–2009 (MOA2009) image map, version 1.

Holland, P. R., Brisbourne, A., Corr, H. F. J., McGrath, D., Purdon, K., Paden, J., et al. (2015). Atmospheric and oceanic forcing of Larsen C Ice Shelf thinning. *The Cryosphere Discussions*, *9*, 251–299. https://doi.org/10.5194/tcd-9-251-2015

Holland, P. R., Corr, H. F. J., Pritchard, H. D., Vaughan, D. G., Arthern, R. J., Jenkins, A., & Tedesco, M. (2011). The air content of Larsen Ice Shelf. *Geophysical Research Letters*, *38*, L10503. https://doi.org/10.1029/2011GL047245

Hubbard, B., Luckman, A., Ashmore, D. W., Bevan, S., Kulessa, B., Kuipers Munneke, P., et al. (2016). Massive subsurface ice formed by refreezing of ice-shelf melt ponds. *Nature Communications*, *7*, 11897. https://doi.org/10.1038/ncomms11897

Jenkins, A., Dutrieux, P., Jacobs, S. S., McPhail, S. D., Perrett, J. R., Webb, A. T., & White, D. (2010). Observations beneath Pine Island Glacier in West Antarctica and implications for its retreat. *Nature Geoscience*, *3*, 468–472. https://doi.org/10.1038/ngeo890

Kuipers Munneke, P., Ligtenberg, S. R. M., Van Den Broeke, M. R., & Vaughan, D. G. (2014). Firn air depletion as a precursor of Antarctic ice-shelf collapse. *Journal of Glaciology*, *60*, 205–214. https://doi.org/10.3189/2014jog13j183

Kuipers Munneke, P., Luckman, A. J., Bevan, S. L., Smeets, C. J. P. P., Gilbert, E., van den Broeke, M. R., et al. (2018). Intense winter surface melt on an Antarctic Ice Shelf. *Geophysical Research Letters*, *45*, 7615–7623. https://doi.org/10.1029/2018GL077899

Kuipers Munneke, P., van den Broeke, M. R., King, J. C., Gray, T., & Reijmer, C. H. (2012). Near-surface climate and surface energy budget of Larsen C ice shelf, Antarctic Peninsula. *The Cryosphere*, *6*, 353–363. https://doi.org/10.5194/tc-6-353-2012

Ligtenberg, S. R. M., Helsen, M. M., & van den Broeke, M. R. (2011). An improved semi-empirical model for the densification of Antarctic firn. *The Cryosphere*, *5*, 809–819. https://doi.org/10.5194/tc-5-809-2011

Liu, Y., Moore, J. C., Cheng, X., Gladstone, R. M., Bassis, J. N., Liu, H., Wen, J., & Hui, F. (2015). Ocean-driven thinning enhances iceberg calving and retreat of Antarctic ice shelves. *Proceedings of the National Academy of Sciences*, *112*, 3263–3268. https://doi.org/10.1073/pnas.1415137112

Long, D. G., & Hicks, B. R. (2010). Standard BYU QuikSCAT and Seawinds land/ice image products (Tech. Rep.) Provo, UT 84602: BYU Center for Remote Sensing, Microwave Earth Remote Sensing Laboratory, BYU Center for Remote Sensing, Brigham Young University, 459 Clyde Building.

Luckman, A., Elvidge, A., Jansen, D., Kulessa, B., Munneke, P. K., King, J., & Barrand, N. E. (2014). Surface melt and ponding on Larsen C Ice Shelf and the impact of föhn winds. *Antarctic Science*, *26*, 625–635. https://doi.org/10.1017/s0954102014000339

Marshall, G. J. (2003). Trends in the southern annular mode from observations and reanalyses. *Journal of Climate*, *16*(24), 4134–4143. https://doi.org/10.1175/1520-0442(2003)016%3C4134:titsam%3E2.0.co;2

Matsuoka, K., Hindmarsh, R. C. A., Moholdt, G., Bentley, M. J., Pritchard, H. D., Brown, J., et al. (2015). Antarctic ice rises and rumples: Their properties and significance for ice-sheet dynamics and evolution. *Earth-Science Reviews*, *150*, 724–745. https://doi.org/10.1016/j.earscirev.2015.09.004

Mortin, J., Howell, S. E. L., Wang, L., Derksen, C., Svensson, G., Graversen, R. G., & Schrøder, T. M. (2014). Extending the QuikSCAT record of seasonal melt-freeze transitions over Arctic sea ice using ASCAT. *Remote Sensing of Environment*, *141*, 214–230. https://doi.org/10.1016/j.rse.2013.11.004

Nghiem, S. V., & Tsai, W.-Y. (2001). Global snow cover monitoring with spaceborne K/sub u/-band scatterometer. *IEEE Transactions on Geoscience and Remote Sensing*, *39*(10), 2118–2134. https://doi.org/10.1109/36.957275

Paolo, F. S., Fricker, H. A., & Padman, L. (2015). Volume loss from Antarctic ice shelves is accelerating. *Science*, *348*, 327–331. https://doi.org/10.1126/science.aaa0940

Picard, G., & Fily, M. (2006). Surface melting observations in Antarctica by microwave radiometers: Correcting 26-year time series from changes in acquisition hours. *Remote Sensing of Environment*, *104*, 325–336. https://doi.org/10.1016/j.rse.2006.05.010

Pritchard, H. D., Ligtenberg, S. R. M., Fricker, H. A., Vaughan, D. G., van den Broeke, M. R., & Padman, L. (2012). Antarctic ice-sheet loss driven by basal melting of ice shelves. *Nature*, *484*, 502–505. https://doi.org/10.1038/nature10968

Rignot, E., Mouginot, J., Morlighem, M., Seroussi, H., & Scheuchl, B. (2014). Widespread, rapid grounding line retreat of Pine Island, Thwaites, Smith, and Kohler glaciers, West Antarctica, from 1992 to 2011. *Geophysical Research Letters*, *41*, 3502–3509. https://doi.org/10.1002/2014gl060140

Scambos, T. A., Haran, T. M., Fahnestock, M. A., Painter, T. H., & Bohlander, J. (2007). MODIS-based Mosaic of Antarctica (MOA) data sets: Continent-wide surface morphology and snow grain size. *Remote Sensing of Environment*, *111*, 242–257. https://doi.org/10.1016/j.rse.2006.12.020

Scambos, T. A., Hulbe, C., Fahnestock, M., & Bohlander, J. (2000). The link between climate warming and break-up of ice shelves in the Antarctic Peninsula. *Journal of Glaciology*, *46*(154), 516–530. https://doi.org/10.3189/172756500781833043

Sergienko, O., & Macayeal, D. R. (2005). Surface melting on Larsen Ice Shelf, Antarctica. *Annals of Glaciology*, *40*, 215–218. https://doi.org/10.3189/172756405781813474

Tedesco, M. (2009). Assessment and development of snowmelt retrieval algorithms over Antarctica from K-band spaceborne brightness temperature (1979-2008). *Remote Sensing of Environment*, *113*, 979–997. https://doi.org/10.1016/j.rse.2009.01.009

Torinesi, O., Fily, M., & Genthon, C. (2003). Variability and trends of the summer melt period of Antarctic ice margins since 1980 from microwave sensors. *Journal of Climate*, *16*(7), 1047–1060. https://doi.org/10.1175/1520-0442(2003)016%3C1047:vatots%3E2.0.co;2

Trusel, L. D., Frey, K. E., & Das, S. B. (2012). Antarctic surface melting dynamics: Enhanced perspectives from radar scatterometer data. *Journal of Geophysical Research*, *117*, F02023. https://doi.org/10.1029/2011JF002126

Trusel, L. D., Frey, K. E., Das, S. B., Karnauskas, K. B., Kuipers Munneke, P., van Meijgaard, E., & van den Broeke, M. R. (2015). Divergent trajectories of Antarctic surface melt under two twenty-first-century climate scenarios. *Nature Geoscience*, *8*, 927–932. https://doi.org/10.1038/ngeo2563

Turner, J., Lu, H., White, I., King, J. C., Phillips, T., Hosking, J. S., et al. (2016). Absence of 21st century warming on Antarctic Peninsula consistent with natural variability. *Nature*, *535*, 411–415. https://doi.org/10.1038/nature18645

van Wessem, J. M., van de Berg, W. J., Noël, B. P. Y., van Meijgaard, E., Amory, C., Birnbaum, G., et al. (2018). Modelling the climate and surface mass balance of polar ice sheets using RACMO2 Part 2: Antarctica (1979–2016). *The Cryosphere*, *12*, 1479–1498. https://doi.org/10.5194/tc-12-1479-2018

van den Broeke, M. (2005). Strong surface melting preceded collapse of Antarctic Peninsula ice shelf. *Geophysical Research Letters*, *32*, L12815. https://doi.org/10.1029/2005GL023247

van den Broeke, M., König-Langlo, G., Picard, G., Kuipers Munneke, P., & Lenaerts, J. (2009). Surface energy balance, melt and sublimation at Neumayer Station, East Antarctica. *Antarctic Science*, *22*, 87–96. https://doi.org/10.1017/s0954102009990538

Vaughan, D. G. (2006). Recent trends in melting conditions on the antarctic peninsula and their implications for ice-sheet mass balance and sea level. *Arctic Antarctic and Alpine Research*, *38*, 147–152. https://doi.org/10.1657/1523-0430(2006)038%5B0147:rtimco%5D2.0.co;2

Wiesenekker, J., Munneke, P. K., van den Broeke, M., & Smeets, C. (2018). A multidecadal analysis of Föhn winds over Larsen C ice shelf from a combination of observations and modeling. *Atmosphere*, *9*, 172. https://doi.org/10.3390/atmos9050172

Wismann, V. (2000). Monitoring of seasonal snowmelt on Greenland with ERS scatterometer data. *IEEE Transactions on Geoscience and Remote Sensing*, *38*(4), 1821–1826. https://doi.org/10.1109/36.851766